Simulation of Orbital Perturbations and Conjunction Analysis Using MATLAB

Theo Altneu, Junil Lee, Ivan Mak, Ethan Olson
University of Arizona Aerospace and Mechanical Engineering
Course Number: AME 557

Abstract

The topics discussed in this report build capabilities and methods for describing the behavior of an orbit. First, we develop a function for converting between orbit elements and inertial state vectors. Then we develop a framework for propagating an orbit under conservative and nonconservative perturbations such as J2 perturbation due to the oblateness of the Earth and atmospheric drag, noting secular changes to key orbital parameters such as RAAN. Finally, these methods are applied to a simulation of the ISS to determine characteristics of conjunction between the ISS and another satellite in a neighboring orbit. Knowing the epochs of conjunction gives information about where and when to make optical observations of the neighboring satellite from the ISS.

Introduction

This report investigates satellite motion and its applications to mission design, focusing on the development of computational tools and simulations using MATLAB to model orbital dynamics. The project is divided into three tasks, each building upon the previous, to describe aspects of orbital mechanics, from the conversion of orbital elements to the simulation of satellite motion under perturbative forces and conjunction analysis between two spacecrafts.

The first task, done by Junil, involves developing a MATLAB subroutine to convert between classical orbital elements and position/velocity vectors. This MATLAB subroutine is fundamental for the following two tasks as it allows for geometric interpretations of a particular orbit by transitioning between the two representations. The subroutine manages both elliptical and hyperbolic orbits, and its accuracy was verified through conversions in both directions, and a comparison to established test cases, using Kepler's equation and Newton's method. This tool serves as the foundation for more complicated orbital simulations.

Task two, done by Ivan, the task one subroutine is used to simulate an arbitrary satellite orbit under both unperturbed and perturbed conditions. Using MATLAB's ode45 solver, an unperturbed two-body simulation was first performed and validated by inspecting the orbit energy, angular momentum, and orbit elements. The simulation was then expanded to include the J2 perturbation caused by Earth's oblateness. This introduced periodic and secular changes in the orbital elements, particularly a precession of the right ascension of ascending node (RAAN), while other elements such as eccentricity and inclination experienced periodic variations. Finally, atmospheric drag was incorporated into the simulation. The drag caused the orbit to gradually decay, leading to circularization and a reduction in altitude. This secular change in orbital energy and semi-major axis places an upper bound on mission of life of certain low altitude satellites.

Task three, done by Theo and Ethan, focuses on the ISS and an arbitrary satellite, analyzing the true longitude and close approach points between the bodies. The computation and calculations for this task were done through MATLAB and uses the task one subroutine to convert orbital elements to inertial states and vice versa. Due to the nature of the subtasks building off each other, it made the most sense to build everything into one function. Using fundamentals of orbital mechanics, the two body equations of motion, with and without the J2 perturbation, can be managed by ode45 with set initial conditions. The data returned by ode45 is then extracted for the necessary subtask calculations. With true longitude in mind, the states, and orbital elements of each body at every time step are extracted. The task one subroutine can once again be used to convert the states at every step to orbital elements. Furthermore, the necessary calculations can be made inside of the loop to complete all subtasks and are explained in detail in the methods section. Figures are produced using calculated data which can be used for analysis, confirming whether the simulations confirm expected trends and data.

Methods

Conversion Between Inertial State and Orbital Elements

There exists a formulaic process for converting between inertial states and orbital elements. However, the process depends on whether the orbit is elliptical or hyperbolic because of having to solve different forms of Kepler's Equation [1] [2]. Thus, we discuss two different methods for ellipses and hyperbolas. Equations 1 and 2 calculate the mean anomaly after the given time using Kepler's equation:

$$\text{(ellipse) } M = M0 + \sqrt{\frac{\mu}{a^3}} * \Delta t \quad (1)$$

$$\text{(hyperbola) } Mh = M0 + \sqrt{\frac{\mu}{(-a^3)}} * \Delta t \quad (2)$$

With mean anomaly, we solve for the eccentric/hyperbolic anomaly iteratively by Newton's method [1] using Equations 3 and 4.

$$\text{(ellipse) } E_{i+1} = E_i - \frac{E_i - e*\sin(E_i) - M}{1 - e*\cos(E_i)} \quad (3)$$

$$\text{(hyperbola) } H_{i+1} = H_i - \frac{e*\sinh(H_i) - H_i - Mh}{e*\cosh(H_i) - 1} \quad (4)$$

Afterwards, we calculate the true anomaly, which also yields the position and velocity vectors in perifocal coordinates using Equations 5 through 8.

$$\text{(ellipse) } \nu = 2\tan^{-1}\left[\sqrt{\frac{1+e}{1-e}}\tan\frac{E}{2}\right] \quad (5)$$

$$\text{(hyperbola) } \nu = 2\tan^{-1}\left[\sqrt{\frac{e+1}{e-1}}\tanh\frac{H}{2}\right] \quad (6)$$

$$\boldsymbol{r}^p = [rcos\nu;\ \ rsin\nu;\ \ 0] \quad (7)$$

$$\boldsymbol{v}^p = \left[-\sqrt{\frac{\mu}{p}}sin\nu;\ \ \sqrt{\frac{\mu}{p}}(e + cos\nu);\ \ 0\right] \quad (8)$$

Finally, a DCM matrix (Equation 9) using the remaining orbital elements transforms the vectors into the ECI (Earth-Centered Inertial) frame.

$$[NP] = \begin{bmatrix} \cos\Omega\cos w - \sin\Omega\sin w\cos i & -\cos\Omega\sin w - \sin\Omega\cos w\cos i & \sin\Omega\sin i \\ \sin\Omega\cos w + \cos\Omega\sin w\cos i & -\sin\Omega\sin w + \cos\Omega\cos w\cos i & -\cos\Omega\sin i \\ \sin w\sin i & \cos w\sin i & \cos i \end{bmatrix} \quad (9)$$

$$\boldsymbol{r}^N = [NP]\cdot\boldsymbol{r^p},\ \boldsymbol{v}^N = [NP]\cdot\boldsymbol{v}^p \quad (10)$$

RV to OE Conversion:

As there exists a formulation from orbital elements to state vectors, the same is true for the reverse.

$$\| \overline{r} \| = \overline{r}\cdot\overline{r},\ \ \| \overline{v} \| = \overline{v}\cdot\overline{v} \quad (11)$$

These transformations start with calculating the specific angular momentum, eccentricity vector and ascending node vector (Equations 13-15). The semi-major axis can also be calculated by rearranging the equation for specific energy, thus finishing one sixth of the classical orbital elements set.

$$a = \frac{-\mu}{2\varepsilon},\qquad \varepsilon = \frac{v^2}{2} - \frac{\mu}{r} \quad (12)$$

$$\overline{h} = \overline{r}\times\overline{v} \quad (13)$$

$$\overline{e} = \frac{\overline{v}\times\overline{h}}{\mu} - \frac{\overline{r}}{r} \quad (14)$$

$$\overline{n} = \overline{K}\times\overline{h} \quad (15)$$

Determining the classical orbital elements from the position and velocity vectors then becomes trivial. The nature of trigonometric functions brings quadrant checks into question; this introduces the use of atan2 which accounts for the correct quadrant. The completion of this reverse formulation completes the subroutine, and it can now be called in other functions to convert state vectors to orbital elements or vice versa.

$$i = \cos^{-1}\left(\frac{\overline{h}\cdot\overline{K}}{h}\right) \quad (16)$$

$$\Omega = atan2\left(\overline{n}\cdot\overline{J}, \overline{n}\cdot\overline{I}\right) \quad (17)$$

$$w = atan2\left(\overline{e}\cdot\left(\overline{h}\times\overline{n}\right), h*\left(\overline{e}\cdot\overline{n}\right)\right) \quad (18)$$

$$\nu = \cos^{-1}\left(\frac{\overline{e}\cdot\overline{r}}{er}\right), \left(\overline{r}\cdot\overline{v}\geq 0\right) \quad (19)$$

$$\nu = 2\Pi - \cos^{-1}\left(\frac{\overline{e}\cdot\overline{r}}{er}\right), \left(\overline{r}\cdot\overline{v}< 0\right) \quad (20)$$

General Orbit Simulation

Unperturbed Orbit Simulation

Developing a simulation for an unperturbed orbit requires choosing appropriate equations of motion and then resolving them into state space for use in numerical integrator's such as MATLAB's 'ode45' function. The acceleration of a spacecraft about a central body is described in Equation 21:

$$\ddot{\vec{r}} = -\frac{u}{r^3}\vec{r} \quad (21)$$

Resolving this into state space gives the components of the acceleration vector in Equations 22 through 24:

$$\ddot{x} = -\frac{\mu x}{r^3} \quad (22)$$

$$\ddot{y} = -\frac{\mu y}{r^3} \quad (23)$$

$$\ddot{z} = -\frac{\mu z}{r^3} \quad (24)$$

The equations of motion, in addition to the initial conditions of interest, enable simulation of any unperturbed orbit.

Orbit Simulation with J2 Perturbation

The unperturbed equations of motion adequately model motion about a spherical central body. However, a more realistic model of the Earth considers it as an oblate spheroid. For applications sensitive to RAAN (Ω), the J2 perturbation may be important to consider. To modify the unperturbed equations of motion to account for J2 perturbation, it is treated as a disturbing potential, such that the potential energy of the spacecraft has the form in Equation 25:

$$U(\vec{r}) = \frac{\mu}{r} + R(\vec{r}) \quad (25)$$

The corresponding disturbing potential due to the oblateness of the Earth [1] is:

$$R = -\frac{\mu}{r}J_2\left(\frac{R_E}{r}\right)^2\frac{3}{2}\left(\left(\frac{z}{r}\right)^2 - \frac{1}{3}\right) \quad (26)$$

Taking the derivative of the disturbing potential with respect to the position vector gives the equations of motion for a J2 perturbed orbit *[3, 4]*:

$$\ddot{x} = -\frac{\mu x}{r^3}\left(1 - J_2\frac{3}{2}\left(\frac{R_E}{r}\right)^2\left(\frac{5z^2}{r^2} - 1\right)\right) \quad (27)$$

$$\ddot{y} = -\frac{\mu y}{r^3}\left(1 - J_2\frac{3}{2}\left(\frac{R_E}{r}\right)^2\left(\frac{5z^2}{r^2} - 1\right)\right) \quad (28)$$

$$\ddot{z} = -\frac{\mu z}{r^3}\left(1 - J_2\frac{3}{2}\left(\frac{R_E}{r}\right)^2\left(\frac{5z^2}{r^2} - 3\right)\right) \quad (29)$$

Thus, through Equations 27-29, a J2 perturbed orbit may be simulated numerically.

Orbit Simulation with Atmospheric Drag

A significant perturbation for spacecraft orbits in Low Earth Orbit (LEO) stems from atmospheric drag, which imparts a force on the spacecraft due to its ballistic characteristics and relative motion between the spacecraft and the fluids that make up Earth's atmosphere. A familiar form for the drag acceleration is shown in Equation 30:

$$\bar{a}_D = \frac{1}{2}\frac{C_d A}{m}\rho v_{rel}^2\frac{\bar{v}_{rel}}{v_{rel}} \quad (30)$$

Breaking down this equation into its constituents, the coefficient of drag (C_d), mass (m), and surface area acting normal to the fluid flow (A) are given in Table 8. Next, the atmospheric density depends on the altitude of the spacecraft, so an exponential form for the density is assumed in Equation, with assumed values shown in Table 7.

$$\rho(\vec{r}) = \rho_0 e^{-\frac{\vec{r}-r_0}{H}} \quad (31)$$

Finally, it is important to note that drag acceleration depends on relative velocity [2], not the absolute velocity of the spacecraft, $\frac{d\vec{r}}{dt}$. So instead, the relative velocity is used, $\bar{v}_{rel} = \frac{d\vec{r}}{dt} - \bar{\omega}_E \times \bar{r}$, yielding the components of relative velocity:

$$\bar{v}_{rel} = \begin{bmatrix} v_x + \omega_E y, & v_y - \omega_E x, & v_z \end{bmatrix}^T \quad (32)$$

Then, the components of drag acceleration are readily known as:

$$a_{D,x} = -\frac{1}{2}\frac{C_d A}{m}\rho v_{rel}^2\frac{v_x + \omega_E y}{v_{rel}} \quad (33)$$

$$a_{D,y} = -\frac{1}{2}\frac{C_d A}{m}\rho v_{rel}^2\frac{v_y - \omega_E x}{v_{rel}} \quad (34)$$

$$a_{D,z} = -\frac{1}{2}\frac{C_d A}{m}\rho v_{rel}^2\frac{v_z}{v_{rel}} \quad (35)$$

Adding the components of drag acceleration to their corresponding components of acceleration in a J2 perturbed orbit now allows the same numerical methods to model a spacecraft's orbit as perturbed by both J2 and atmospheric drag.

True Longitude Analysis Between the ISS and a Satellite

Task three focuses on the close approach distances and intervals between the ISS and a given satellite. The ISS is subject to many perturbations, most of which this paper does not cover. Thus, the initial conditions and equations of motion must be chosen appropriately to accurately simulate an ISS orbit without perturbation and with the J2 perturbation. The ISS state vectors used in this report come from ephemeris ISS trajectory data published by ISS Trajectory Operations and Planning Officer Flight

Controllers [3]. The other satellite is stated to be in the same orbit plane as the ISS with a different semi-major axis, eccentricity, and argument of perigee.

Using 'OE_RV_Converter' subroutine created in task one, the ISS states taken from the ephemeris are converted to orbital elements, and then used to find the satellites orbital elements. The difference in argument of perigee between the ISS and the satellite is given as $\Delta\omega = \omega_{sat} - \omega_{ISS} = 233.1°$. With the initial true longitudes at t0 being $\lambda_{true} = 100.5°$ for the ISS and $\lambda_{true} = 355.4°$ for the Satellite.

$$\upsilon = \lambda_{true} - \Omega - \omega \quad (36)$$

$$\tan\frac{E}{2} = \sqrt{\frac{e-1}{e+1}}\tan\frac{\upsilon}{2} \quad (37)$$

$$M = E - e\sin E \quad (38)$$

A few preliminary calculations must be made to set up the code for the subtasks. True longitude can be defined as the sum of true anomaly, argument of perigee, and right ascension of the ascending node [4]. The true anomaly of each body is calculated by rearranging the equation for true longitude, because the argument of perigee and RAAN are known values (Equation 36). Using the equation for eccentric anomaly and Kepler's equation, the true anomaly is used to find the mean anomaly of each orbit (Equations 37-38). This computed mean anomaly then finishes the orbital element set for the respective bodies.

A few preliminary calculations must be made to set up the code for the subtasks. True longitude can be defined as the sum of true anomaly, argument of perigee, and right ascension of the ascending node [4]. The true anomaly of each body is calculated by rearranging the equation for true longitude, because the argument of perigee and RAAN are known values. Using the equation for eccentric anomaly and Kepler's equation, the true anomaly is used to find the mean anomaly of each orbit. This computed mean anomaly then finishes the orbital element set for the respective bodies.

Orbital Elements	ISS	Satellite
a [km]	6793.9270	10349.8
E	0.0019204	0.0934
i [deg]	51.7588	51.7588
Ω [deg]	64.0224	64.0224
ω [deg]	94.4455	327.5455
M [deg]	302.2186	329.8052

Table 1. Task 3 Orbital Elements

Unperturbed Orbits

Subtask one asks for the average interval between times of conjunction between the ISS and the Satellite. A time of conjunction is a time where the ISS and the Satellite share the same true longitude, and where the position vectors are pointing in the same direction. Ode45 is used to integrate the equations of motion for both the ISS and Satellite, with the initial conditions being set based on the orbital elements calculated previously. The equations of motion used in the function, managed by Ode45, are the unperturbed two body equations of motion (Equation 21) in state space form.

Given output data from ode45, in the form of an array with rows spanning the length of the time vector, the true longitude at each time step is calculated. With the use of a for loop, the state vectors are extracted at each time step for each satellite and then converted to orbital elements using the task one subroutine. The returned array includes two thirds of what is needed to find the true

longitude at each step, being the RAAN and argument of perigee. Within this loop, the vectors and magnitudes of the position and velocity of the two bodies are extracted as well. These states are used to calculate the angular momentum vector and eccentricity vector. Finally true anomaly is calculated at each step using equation 39, [2]. With the true anomaly at each time step, the true longitude can now be calculated and plotted against time for comparison.

$$\nu = atan2(\boldsymbol{r} \cdot \boldsymbol{h} \times \boldsymbol{e}\,, h\boldsymbol{r} \cdot \boldsymbol{e}) \quad (39)$$

Where:

$$\boldsymbol{h} = \boldsymbol{r} \times \boldsymbol{v} \quad (40)$$

$$\boldsymbol{e} = \frac{1}{\mu}(\boldsymbol{v} \times \boldsymbol{h}) - \frac{\boldsymbol{r}}{r} \quad (41)$$

As mentioned earlier, the true longitude conjunction points are also defined by where the bodies have position vectors pointing in the same direction. This is directly correlated with the distance between the satellites, with the closest approaches being the conjunction points. This distance between the satellites is easily computed using the magnitude of the difference of the position vectors at each time step. **X = islocalmin(Y)** returns a logical array of zeros, and ones(true) where the local minimums exist in the **Y**. For example, using the position difference data as an input, the output returns a zero filled array with ones where the minimum distances are recorded. Indexing the output with the time array returns the time steps where each minimum distance happens. Extending the simulation to run over the course of over ten orbits will return satisfactory data to calculate the average time between conjunction points, using the method discussed.

It is expected, due to the definition of true longitude, that the conjunctions in true longitude as calculated by the sum of specific elements at each time step should match with the close approaches within the distances of the satellites. Subtask two asks for the minimum and maximum distances between the ISS and satellite at the conjunction points. The setup for this is straightforward using the data collected in subtask one. Given an array of conjunction data points in terms of the distances between satellites, the minimum and maximum of this data is easily obtained using MATLAB functions min and max.

Subtask three asks for the average time interval between successive close approaches at the minimum distance calculated in subtask two. To find the average time, the length of the simulation must be long enough to capture multiple minimum distance close approaches. 50 ISS orbits return ample data. Like subtask one, the function ‘islocalmin’ is used to return the locations of the minimum close approaches within the close approach data obtained in task one. The output array is used with the time vector to return the points in the time vector where these minimum close approaches happen.

Subtask four requests the time after t0 of the first two close approaches at minimum distance. Using the time vector to index the array containing the locations of the minimum close approaches, the times from t0 of the first two close approaches are found easily.

Repeated Numerical Simulation Including J2 Perturbation

Subtask five presents a perturbation to the equations of motion, specifically J2. The J2 perturbation represents the oblateness of Earth and is one of the stronger perturbations. The value of J2 for earth is 0.0010826269. The RAAN, argument of perigee, and mean anomaly are the only orbital elements which see secular change due to J2, so it should be expected to see these changes in the data produced by the code.

To accurately represent the J2 perturbation in the simulations, the equations of motion managed by ode45 must be changed to the appropriate equations in state space form (Equations 27-29). The direction of the J2 acceleration is neither in the position nor velocity direction, which causes the orbit to preces. In turn, the angular momentum vector also changes direction and is no longer conserved. However, the z component of the angular momentum is conserved.

Results and Discussion

Task One

Translate OE to RV and RV to OE in Elliptical/Hyperbolic Orbit

The OE_RV_Converter MATLAB subroutine successfully translates between orbital elements and position/velocity vectors for both elliptic and hyperbolic orbits. The iterative method used to solve Kepler's equation ensures accurate results, and the function was validated by converting both ways on provided both elliptical/hyperbolic cases.

Translate OE to RV and RV to OE in Elliptical Orbit

a (km)	8000	**Rx (km)**	-1264.607
E	0.1	**Ry (km)**	8013.809
i (deg)	30	**Rz (km)**	-3371.251
Ω (deg)	145	**Vx (km/s)**	-6.03962
ω (deg)	120	**Vy (km/s)**	-0.2043976
M0 (deg)	10	**Vz (km/s)**	2.096715

Table 2. Elliptical Orbital Elements to Position/Velocity

Rx (km)	-1264.61	**a (km)**	7999.652
Ry (km)	8013.81	**e**	0.10004
Rz (km)	-3371.25	**i (deg)**	29.9974
Vx (km/s)	-6.03962	**Ω (deg)**	145.0061
Vy (km/s)	-0.204398	**ω (deg)**	120.01539
Vz (km/s)	2.09672	**M0 (deg)**	9.964

Table 3. Elliptical Position/Velocity to Orbital Elements

Translate OE to RV and RV to OE in Hyperbolic Orbit

a (km)	-8000	**Rx (km)**	18876.969
E	1.1	**Ry (km)**	27406.5548
i (deg)	30	**Rz (km)**	-19212.785
Ω (deg)	145	**Vx (km/s)**	3.5596768
ω (deg)	120	**Vy (km/s)**	6.3553158
M0 (deg)	10	**Vz (km/s)**	-4.1844712

Table 4. Hyperbolic Orbital Elements to Position/Velocity

Rx (km)	18877	**a (km)**	-7999.9849
Ry (km)	27406.6	**e**	1.1000
Rz (km)	-19212.8	**i (deg)**	29.99997
Vx (km/s)	3.55968	**Ω (deg)**	144.99991
Vy (km/s)	6.35532	**ω (deg)**	120.0001
Vz (km/s)	-4.18447	**M0 (deg)**	10.00026

Table 5. Hyperbolic Position/Velocity to Orbital Elements

The results contained in Tables 2 through 5 agree with the test case results from Butcher [2].

Task Two

Unperturbed Orbit Simulation

Using the content outlined in Unperturbed Orbit Simulation, we can model the unperturbed orbit of a spacecraft given the initial conditions given in Table 6. The 2D and 3D plots in Figure 1 depict a low eccentricity (near circular) orbit about the Earth at an $63.4°$ inclination. When plotted against time, the eccentricity remains close to zero for the duration of the simulation, further indicating that the given orbit is near circular.

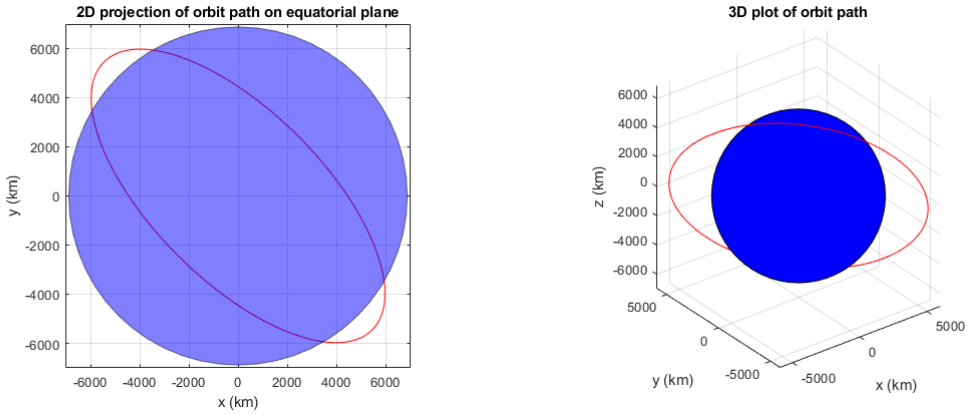

Figure 1. Projection of unperturbed orbit on XY plane in ECI frame (left) and 3D plot of unperturbed orbit in ECI frame (right). The shapes correspond to a circular orbit at an inclination of $63.4°$.

For an unperturbed orbit, we expect the first 5 orbital elements to remain constant, which is also reflected in the Unperturbed Plots of Appendix A: Perturbed and Unperturbed Motion Plots. The true anomaly progresses linearly with time, which agrees with a near circular orbit, since the angular velocity is always constant. Similarly, we can validate the results by plotting the total energy and angular momentum of the system in Figure 2. As expected, these quantities remain constant (the errors are close to numerical precision) for the duration of the simulation since all motion occurs about the gravitational potential of a perfect sphere.

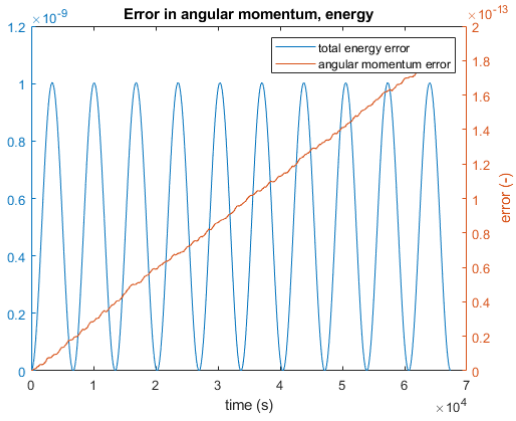

Figure 2. The error in total energy and angular momentum remains constant throughout the course of the simulation, reflecting the sole influence of a conservative gravitational potential.

Orbit Simulation with J2 Perturbation

We apply the methods described for J2 perturbation to demonstrate how a J2 perturbed orbit differs from an unperturbed one. The 2D and 3D plots in Figure 3 show again a low eccentricity orbit

about the Earth at an inclination of $63.4°$. However, the orbit is seen precessing about the Z axis, indicating a secular drift in the orbit's RAAN angle.

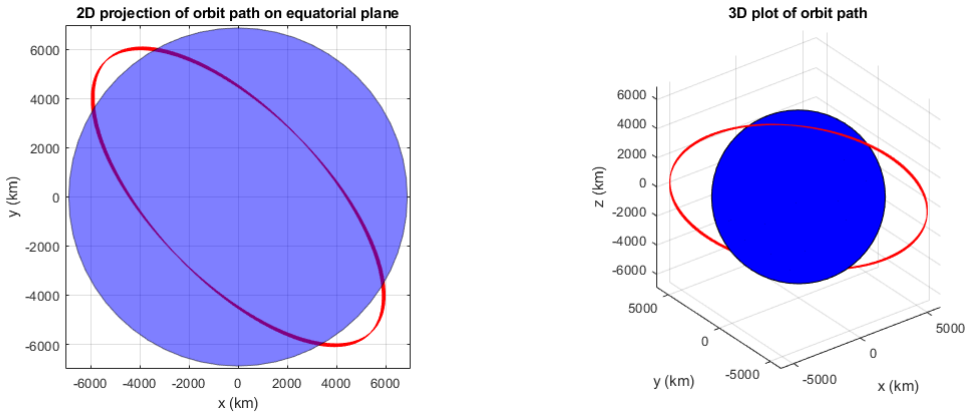

Figure 3. Projection of unperturbed orbit on XY plane in ECI frame (left) and 3D plot of unperturbed orbit in ECI frame (right). Thicker bands in the orbit path reflect a slow Z axis precession of the orbital plane.

Since the perturbation can be modeled as a disturbing potential, we expect the total energy of the system to be conserved, which is supported in Figure 4. Plotting the orbital elements in the J2 Perturbed Plots of Appendix A: Perturbed and Unperturbed Motion Plots reiterates the secular drift in the RAAN angle over time, explaining the precession seen in Figure 3. Other than the RAAN angle, the orbital elements, ω, i, e, and a experience no secular drift, but undergo periodic changes. In general, J2 does affect ω, but the inclination of $63.4°$ has the special quality of bringing the mean change in ω to 0 [2]. Of note is the progression of the true anomaly, which speeds up and slows down over the course of a period. The J2 perturbation, interpreted as a concentration of Earth's mass near the equator, explains the nonlinear behavior since we expect the spacecraft to speed up when it's near the larger concentration of Earth's mass and slow down when it is farther away.

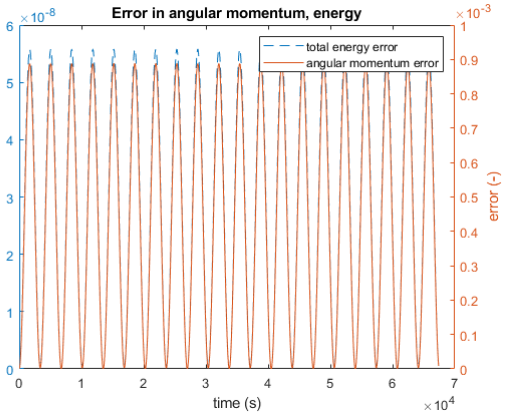

Figure 4. The J2 perturbation manifests periodic changes in the angular momentum and total energy in the orbit. However, no secular drift is present, as expected for a conservative disturbing potential.

Orbit Simulation with J2 Perturbation and Atmospheric Drag

Finally, drag may impact satellites orbiting low enough to interact with the Earth's atmosphere. The simulation is extended to five thousand orbits instead of ten to emphasize drag effects. Figure 5 shows the change in energy, $E - E_0$, which decreases secularly over time, reflecting how drag bleeds

energy from the spacecraft orbit. Since total energy is related to the semi major axis, we expect it to decrease secularly as total energy decreases, as reflected in Figure 17.

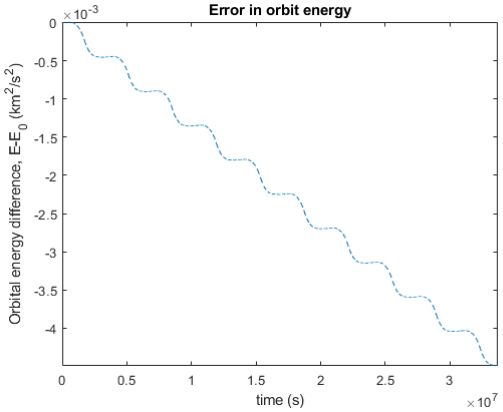

Figure 5. The change in orbital energy experiences both secular and periodic changes. The downward trend occurs since drag continually removes energy from the system.

As seen in the orbital elements plotted in Figure 17 through Figure 19 in Appendix A: Perturbed and Unperturbed Motion Plots, secular drift occurs in the RAAN angle, corresponding to precession of the orbit plane. Argument of periapsis also remains the same due to the specially chosen inclination of $63.4°$, which also remains constant. Eccentricity decreases secularly, reflecting a circularization of the orbit, which should eventually go to zero.

Task Three

Unperturbed Orbital Simulation

Applying the process described in the Methods section, a model for the orbits of the ISS and secondary satellite can be obtained. These orbits are shown in the 2D and 3D plots in the inertial frame in Figure 6.

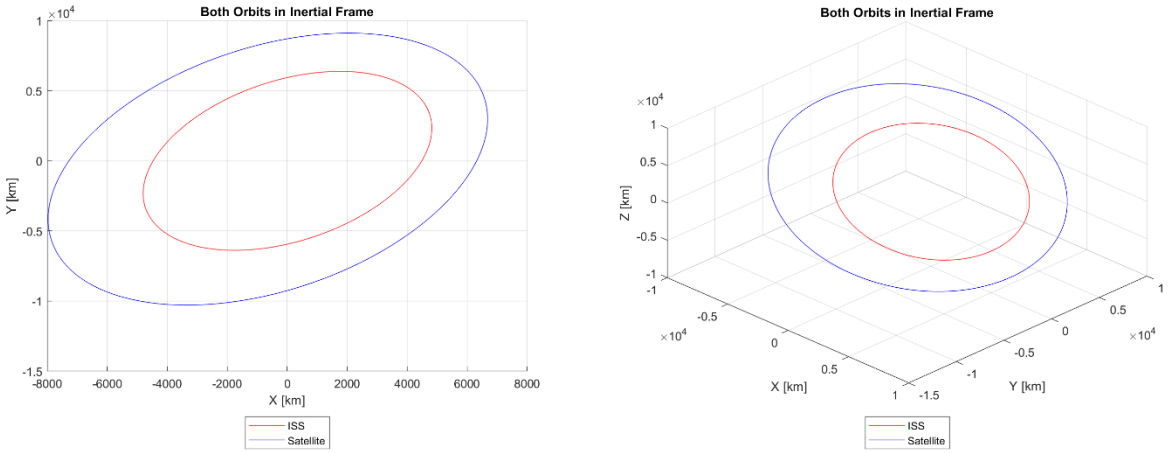

Figure 6. 2D Inertial Frame Orbital Plot (Left), 3D Inertial Frame Orbit Plot (Right)

Given the initial true longitude of 100.5 degrees for the ISS and 355.4 degrees for the satellite, and the orbital elements across the orbital period, the true longitude across the orbit period can also be calculated for both orbits.

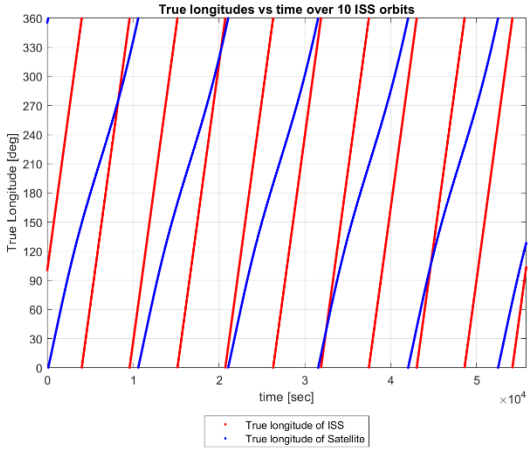

Figure 7. True longitude of orbits over ten orbits

The conjunction points are where true longitude for both the orbits of the ISS and the satellite is the same. The average time between true longitude conjunctions is 11904.0909 seconds, calculated over fifty orbits.

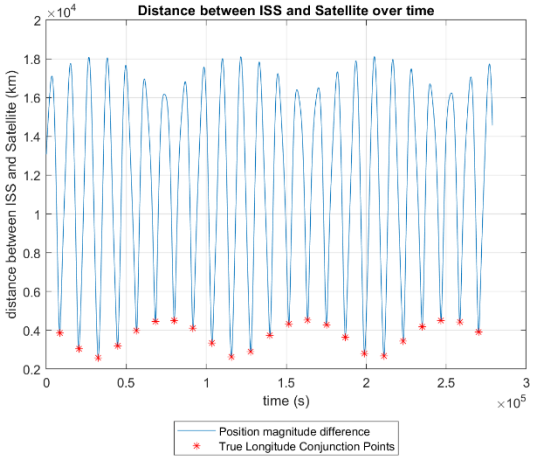

Figure 8. Distance between ISS and satellite over time.

The distance between the ISS and the satellite oscillates, seen in the figure with the true longitude conjunction points. The minimum and maximum distances at conjunction points are 2587.1985 [km] and 4529.5219 [km], respectively. The best time to make optical observations of the satellite from the ISS is during close approaches. The approximate time interval between successive close approaches at the minimum distance is 89325 seconds. The times of the first two close approaches after t0 are 32450 seconds and 115690 seconds, respectively.

Orbital Simulation Including J2 Perturbation

The orbital simulations are conducted with the addition of a J2 perturbation. As a result, the two orbital planes no longer remain identical over time, as the J2 perturbation causes the ISS and the satellite to precess at different rates.

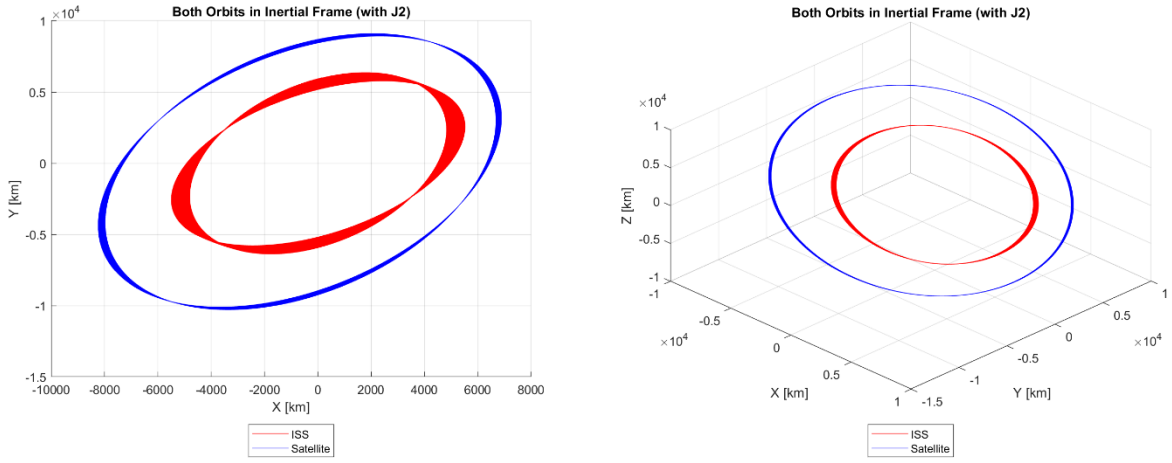

Figure 9. 2D Inertial Frame Orbital Plot (Left), 3D Inertial Frame Orbit Plot (Right) with J2 Perturbation

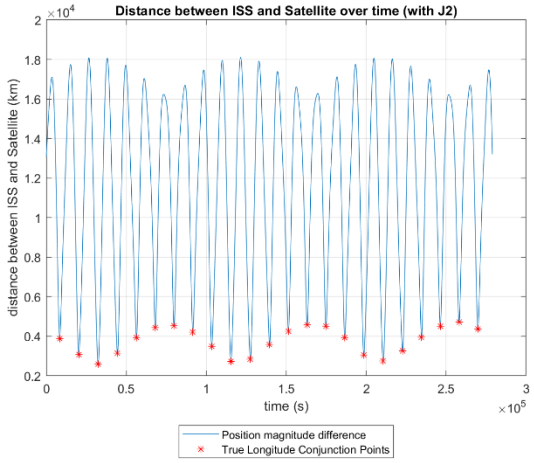

Figure 10. Distance between ISS and satellite over time with J2 perturbation.

The primary concern is the effect on close approaches for optical observations. With a J2 perturbation, the minimum and maximum distances at conjunction are 2589.8359 [km] and 4704.471 [km], respectively. The J2 perturbation slightly increases the minimum distance at conjunction by about 2.5 km, and increases the maximum distance by about 175 km. With a J2 perturbation, the approximate time interval between successive close approaches at the minimum distance is 89110 seconds, which is 215 seconds less than without the J2 perturbation. And finally, with a J2 perturbation, the times of the first two close approaches after t0 are 32380 seconds (70 seconds sooner) and 115430 seconds (260 seconds sooner) respectively. In conclusion, when accounting for the J2 perturbation, the distance at close approaches becomes marginally larger, and the time between close approaches and the time to the first two close approaches becomes marginally closer to the initial time.

Conclusion

In Task 1, MATLAB subroutines were used to convert orbital elements (OE) to position and velocity vectors (RV) and vice versa for elliptical and hyperbolic orbits. The OE to RV conversion involved calculating the mean anomaly, solving for the eccentric or hyperbolic anomaly using Newton's method, and determining the true anomaly to compute the position and velocity vectors, which were then transformed into the ECI frame. The RV to OE conversion used the magnitudes of the position and velocity vectors to calculate key orbital elements, such as semi-major axis, eccentricity, and inclination. Both conversions showed accurate results when compared to given test cases, confirming the validity of the methods for these types of orbits.

In task two, state vectors for an arbitrary orbit were given. Using these state vectors as initial conditions for a numerical integrator, we propagated these orbits under no perturbation, J2 perturbation, and J2 plus atmospheric drag perturbation. The unperturbed orbit considered a near circular orbit, where the total energy of the orbit, as well as five of the orbital elements, remained constant throughout the simulation. J2 perturbation introduced secular changes in the RAAN angle, and periodic changes in all other quantities. Adding atmospheric drag caused energy to bleed from the system, resulting in altitude decay and circularization of the orbit.

Task three simulation results which demonstrate that J2 perturbation introduces minor changes to the relative orbits of the ISS and the secondary satellite. While the J2 perturbation slightly increases the minimum and maximum distances at conjunction by about 2.5 km and 175 km, respectively, it has a negligible effect on period between close approaches for optical observation. The time between successive close approaches is reduced by 215 seconds with perturbation, and the first two close approaches occur marginally earlier. These variations indicate that while J2 perturbation influences the precession of the orbital planes, its impact on close approaches remains minimal. Overall, the J2 perturbation must be considered in precise modeling but does not significantly affect the timing or quality of optical observations from the ISS.

The ability to simulate and observe special characteristics of an orbit occurred in several steps. First, developing methods to convert between inertial state vectors and orbital elements provided geometric perspectives on certain orbits. Then, an arbitrary orbit was simulated under certain unideal conditions such as J2 perturbation and atmospheric drag to demonstrate ability to analyze complex orbit scenarios. Finally, these methods were applied to the case of the ISS and a neighboring satellite to analyze and generate epochs of interest for an observation mission.

References

[1] H. Schaub and J. L. Junkins, Analytical Mechanics of Aerospace Systems, AIAA American Institute of Aeronautics & Ast., 2018.

[2] E. Butcher, "Personal Communication," 2024.

[3] NASA/JSC/FOD/TOPO, *ISS.OEM_J2K_EPH,* 2024.

[4] C. A. Kluever, "Time of Flight," in *Space Flight Dynamics*, John Wiley & Sons Ltd, 2018, pp. 107-146.

[5] D. Vallado and W. Mclain, Fundamentals of Astrodynamics and Applications, Microcosm Press, 2001.

Appendix A: Perturbed and Unperturbed Motion Plots

Unperturbed Plots

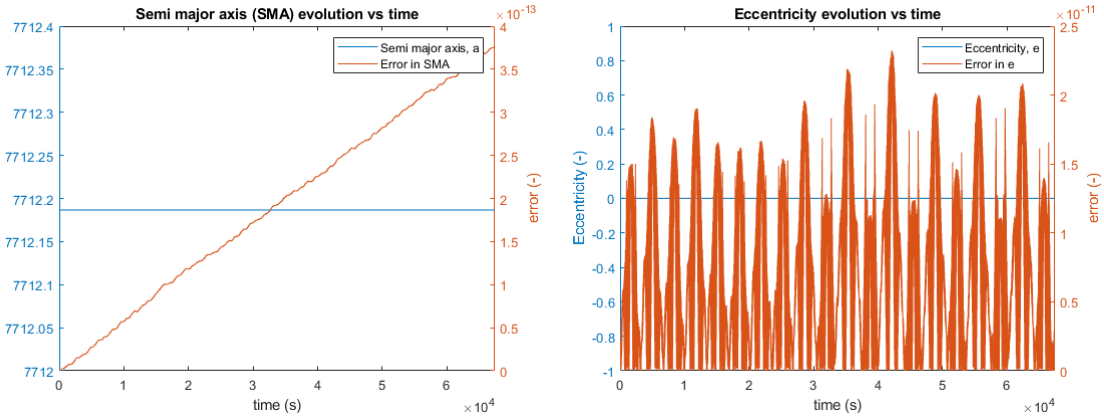

Figure 11. The semi major axis (left) and the eccentricity (right) remain constant over the course of the simulation, as indicated by small errors relative to the initial values.

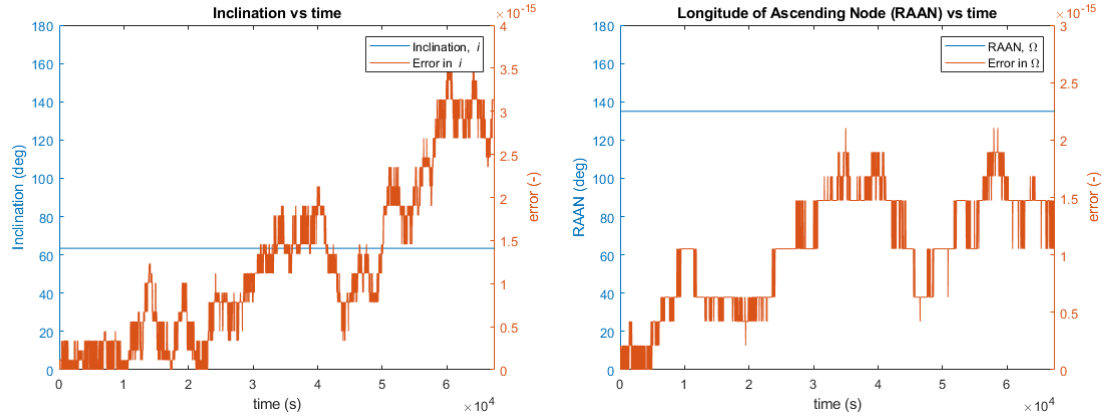

Figure 12. The inclination (left) and RAAN angle (right) remain constant over the course of the simulation, as indicated by small errors relative to the initial values.

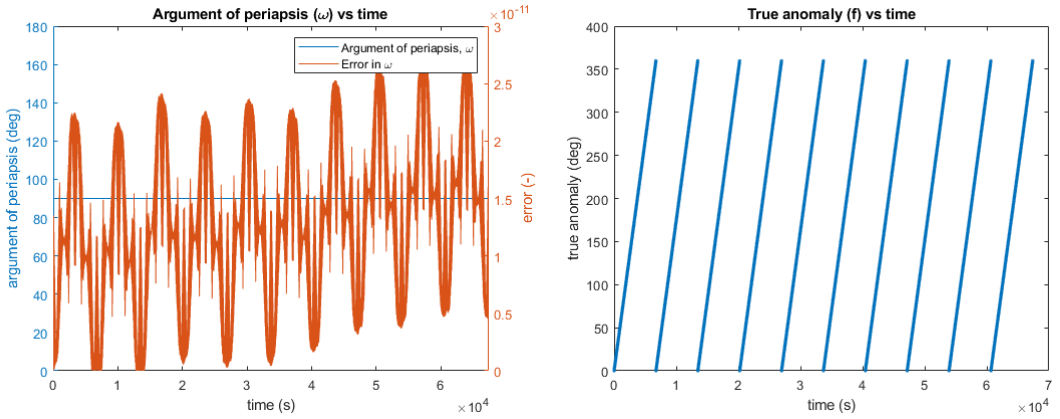

Figure 13. The argument of periapsis (left) remains constant over the course of the simulation, as shown by small errors relative to initial values. True anomaly progresses (right) progresses linearly, as expected of a circular orbit.

J2 Perturbed Plots

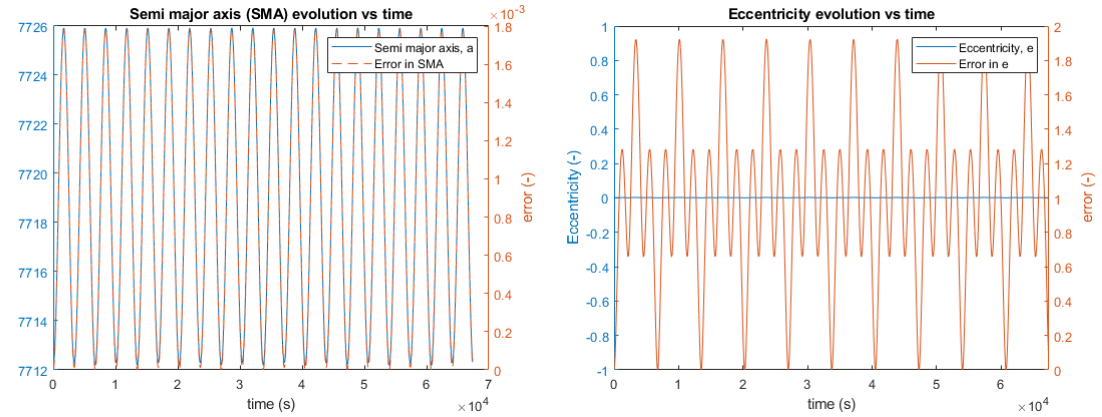

Figure 14. The semi major axis (left) and the eccentricity (right) remain constant over the course of the simulation, as indicated by small errors relative to the initial values.

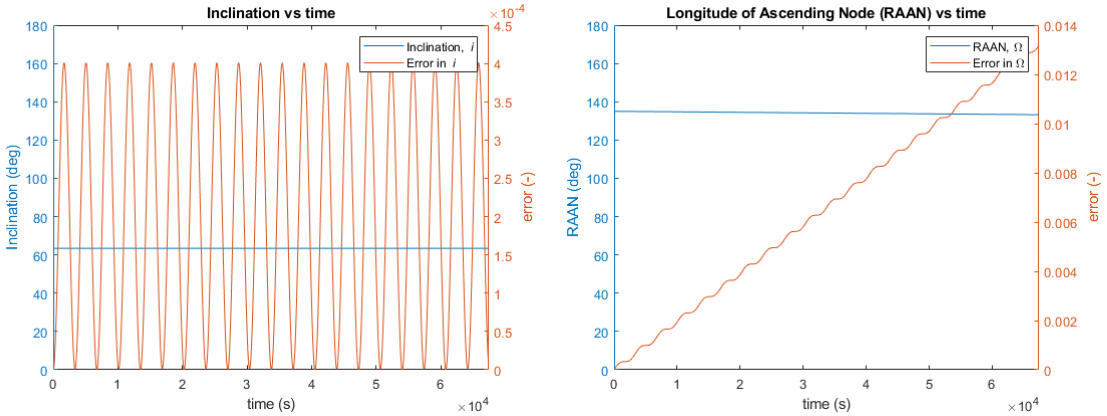

Figure 15. The inclination (left) remains constant over the course of the simulation while the error in RAAN angle (right) increases over time. The RAAN angle error grows with the precession of the ascending node.

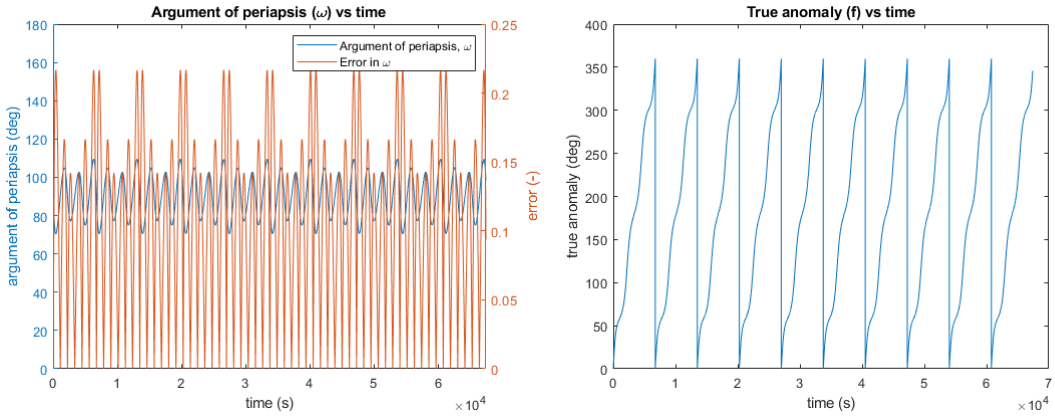

Figure 16. The argument of periapsis (left) remains constant over the course of the simulation due to a specially chosen inclination, as shown by small errors relative to initial values. True anomaly progresses (right) progresses nonlinearly, due to J2 perturbation.

J2 and Atmospheric Drag Perturbed Plots

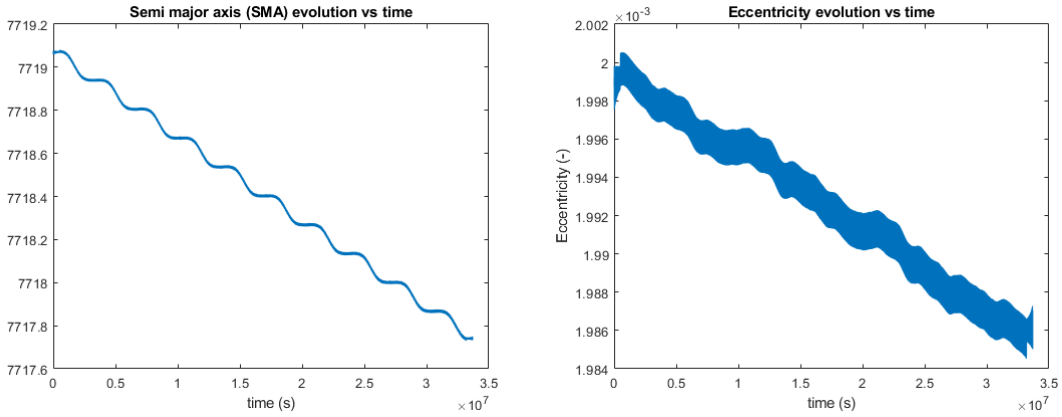

Figure 17. Both the semi major axis (left) and the eccentricity (right) decrease over the course of the simulation. The SMA corresponds to a decrease in orbit energy as the satellite altitude decreases, while the change in eccentricity reflects circularization in the orbit.

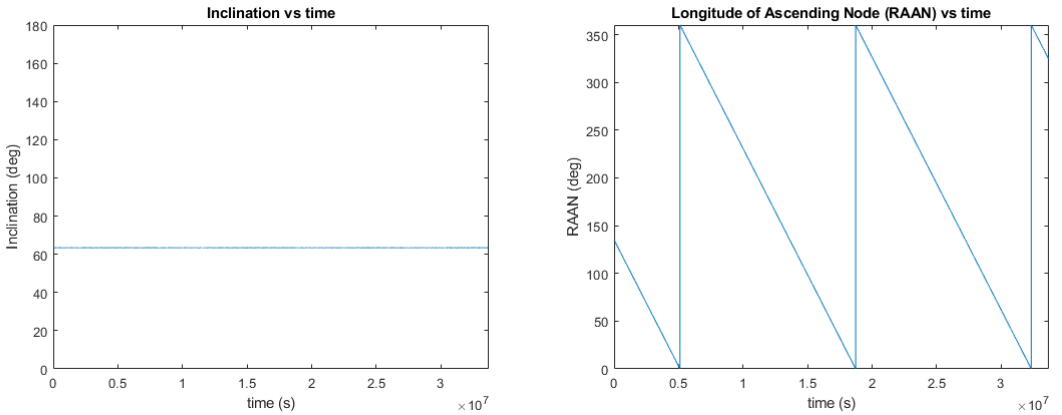

Figure 18. The inclination (left) remains constant throughout the orbit since it is neither affected by atmospheric drag nor J2 perturbation. The RAAN angle precesses multiple revolutions due to J2 perturbation.

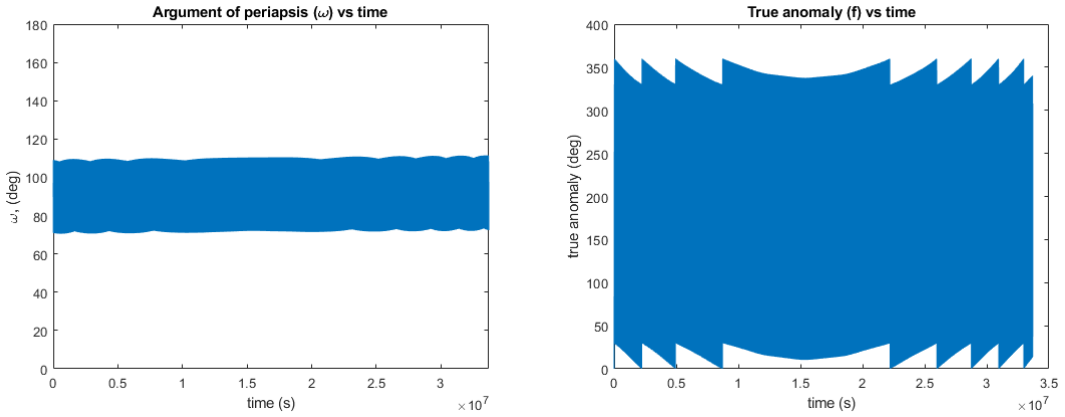

Figure 19. The argument of periapsis (left) remains constant despite the J2 perturbation due to a carefully chosen inclination. The true anomaly is plotted on the right.

Appendix B: Tables

State Vector Component	Value
X position	$-2346.45\ km$
Y position	$-2346.45\ km$
Z position	$6891.0379\ km$
X velocity	$5.088611\ km/s$
Y velocity	$5.088611\ km/s$
Z velocity	$0\ km/s$

Table 6. Initial conditions for the General Orbit Simulation.

Density Function Variable	Value
ρ_0	$4.0 \times 10^{-13}\ kg/m^3$
r_0	$7298.145\ km$
H	$200\ km$

Table 7. Quantities for atmospheric density function.

Aerodynamic Property	Value
C_d	2.0
A	$3.6\ m^2$
m	$1350\ kg$

Table 8. Assumed spacecraft properties for atmospheric drag model.

Equation 42